Chapter 4

Impairment to Optical Signals

The last chapter is the performance of optical receiver in the ideal case limited only by amplifier noises, or shot noise if optical amplifiers are not used. In practice, there are many other noise sources that degrade the performance of the optical receiver.

If the LO laser is very noisy with relative intensity noise, with the single branch receiver of Sec. 3.1.1, the optical signal is very likely to be limited by the LO noise. One of the main advantage of using balanced receiver is to reduce the impact of LO noise. In coherent optical communication, the laser sources must be coherent with very low phase noise. In early studies of coherent optical communication, laser phase noise is a major limitation of the system (Betti et al., 1995, Okoshi and Kikuchi, 1988, Ryu, 1995). Because early system trend to have a low data rate, the ratio of laser linewidth to the data rate is very significant compared with contemporary 10 and 40-Gb/s systems.

When coherent optical signal is transmitted in the optical fiber, the signal is distorted by fiber dispersion and polarization-mode dispersion. Fiber dispersion limits the maximum transmission distance as signal with a wide spectrum with components travel in different speed. As the signal at two orthogonal polarizations along the principle states of polarization has different group delay, polarization-mode dispersion also broaden the signal. This chapter considers only linear fiber effects, the coming three chapters will consider the signal distortion due to fiber nonlinearities.

4.1 Relative Intensity Noise

In the analysis of the single-branch receiver of Sec. 3.1.1, the relative intensity noise (RIN) is included in $n_L(t)$ of Eq. (3.4). As shown in Sec. 3.1.1, if the power of LO laser P_{LO} is much larger than the signal power of P_r. In the photocurrent of Eq. (3.7), the two mean noise sources are LO-spontaneous beat noise and the RIN from $|A_L + n(t)|^2$. Including only LO-spontaneous beat noise and RIN, the SNR of single-branch receiver is

$$\begin{aligned} \rho_s &= \frac{\frac{1}{2}R^2 P_{\mathrm{LO}} P_r}{\frac{1}{2}R^2 P_{\mathrm{LO}} S_{n_s} B_d + \frac{1}{2}R^2 P_{\mathrm{LO}}^2 \sigma_{\mathrm{RIN}}^2} \\ &= \frac{P_r}{S_{n_s} B_d + P_{\mathrm{LO}} \sigma_{\mathrm{RIN}}^2}. \end{aligned} \tag{4.1}$$

where the variance due to RIN is equal to

$$\sigma_{\mathrm{RIN}}^2 = \int_{f_{\mathrm{IF}}-B_d}^{f_{\mathrm{IF}}+B_d} \mathrm{RIN}(f)\mathrm{d}f. \tag{4.2}$$

where the $\mathrm{RIN}(f)$ is the RIN spectrum. With a large LO power of P_{LO}, the impact of RIN is very significant. A expression similar to Eq. (4.1) can also be expressed for balanced receiver, the impact of RIN is drastically reduced with a SNR of

$$\begin{aligned}\rho_s &= \frac{P_r}{S_{n_s}B_d + \frac{1}{2}P_r\hat{\sigma}^2_{\mathrm{RIN}}} \\ &= \frac{\rho_{s0}}{1+\frac{\rho_{s0}}{2}\hat{\sigma}^2_{\mathrm{RIN}}}.\end{aligned} \tag{4.3}$$

where $\rho_{s0} = P_r/S_{n_s}B_d$ is the SNR without RIN and

$$\hat{\sigma}^2_{\mathrm{RIN}} = \int_{-B_d}^{+B_d} \mathrm{RIN}(f)\mathrm{d}f. \tag{4.4}$$

Comparing the SNR of Eq. (4.1) with Eq. (4.3), it is obvious that the impact of RIN to single branch receiver is much larger than that to balanced receiver.

An analysis of the impact of LO noise to single-branch and balanced receiver can be found at Abbas et al. (1985), Alexander (1987), Hodgkinson (1987), Yuen and Chan (1983). If the two branches of the balanced receiver is not symmetry, the LO noise degrades the SNR of the system more than that of Eq. (4.3) (Abbas et al., 1985).

4.2 Phase Errors in Orthogonal Signals

In the heterodyne receiver of DPSK signal in Fig. 1.4(b) and the direct-detection DPSK receiver of Fig. 1.4(c) or Fig. 3.12, the phase delay of the delay-and-multiplier circuit or asymmetry Mach-Zehnder interferometer must equal to integer of 2π. In the heterodyne DPSK receiver of Fig. 1.4(b), we need $\exp(j\omega_{\mathrm{IF}}T) = 1$, where T is the delay of the delay-and-multiplier circuits and approximately equal to the symbol time of the DPSK signal. In the direction-detection DPSK receiver of Fig. 3.12, we also need $\exp(j\omega_c T) = 1$. A phase error is induced into the system if either $\exp(j\omega_{\mathrm{IF}}T) = e^{j\theta_e}$ or $\exp(j\omega_c T) = e^{j\theta_e}$, where $-\pi < \theta_e < +\pi$ is the phase error of the DPSK receiver.

In an alternative description, the interferometer or delay-and-multiplier circuit has their operating frequency. If the path difference does not match to the frequency of the signal, the phase error is equal to $\theta_e = 2\pi\Delta f T$, where Δf is the frequency mismatch.

4.2.1 Delay Phase Error for DPSK Signals

From (Blachman, 1981), the error probability for a DPSK signal with phase error is

$$p_e = \frac{1}{2} - \frac{\rho_s e^{-\rho_s}}{2}\sum_{k=0}^{\infty}\frac{(-1)^k}{2k+1}\left[I_k\left(\frac{\rho_s}{2}\right) + I_{k+1}\left(\frac{\rho_s}{2}\right)\right]^2 \times \cos[(2k+1)\theta_e], \tag{4.5}$$

where $I_k(\cdot)$ is the kth-order modified Bessel function of the first kind. The above error probability of Eq. (4.5) comes almost directly from Eq. (57) of the Appendix. The mth Fourier coefficient of the phase error is obviously equal to $cosm\theta_e$.

From (Ho, 2004), there is simpler formula for the phase error. The polarized direct-detection DPSK receiver is equivalent to heterodyne DPSK receiver. At the output of the balanced receiver, ignoring the constant factor of coupler loss, photodetector responsivity, and receiver gain, the signal is similar to the difference of Eq. (3.152) and Eq. (3.153) but without the noise from orthogonal direction

$$i(t) = \left|E(t) + e^{j\theta_e}E(t-T)\right|^2 - \left|E(t) - e^{j\theta_e}E(t-T)\right|^2. \tag{4.6}$$

As the signal of Eq. (4.6) is the same as that of the decision variable for envelope detection of correlated binary signals of Sec. 3.3.6, the equivalent correlation coefficient is

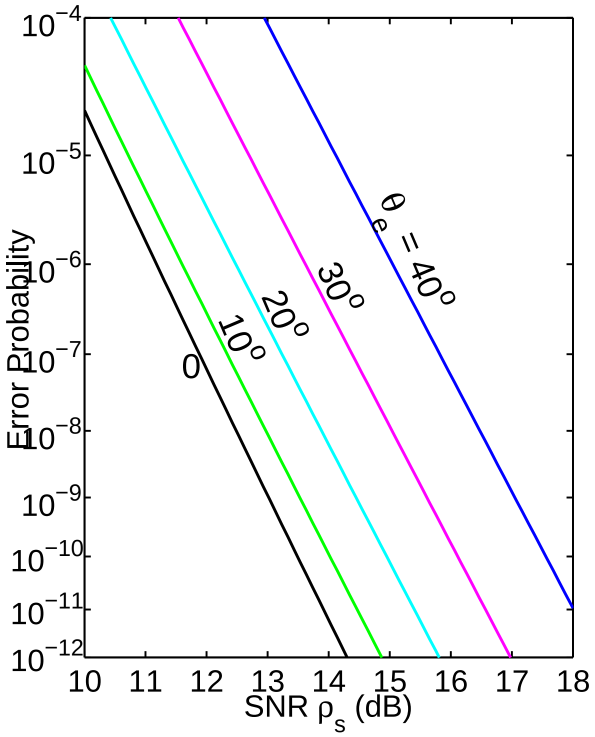

Figure 4.1: BER as a function of SNR ρ_s for DPSK with phase error.

$$\frac{1}{2}\left|1+e^{j\theta_e}\right|\left|1-e^{-j\theta_e}\right| = \sin\theta_e. \tag{4.7}$$

Using Eq. (3.117), the BER is

$$p_e = Q(a,b) - \tfrac{1}{2}e^{-(a^2+b^2)/2}I_0(ab),$$
$$a = \sqrt{2\rho_s}\left|\sin\tfrac{\theta_e}{2}\right|, \quad b = \sqrt{2\rho_s}\left|\cos\tfrac{\theta_e}{2}\right|, \tag{4.8}$$

where $Q(\cdot,\cdot)$ is the well-known first-order Marcum's Q function, and ρ_s is the signal-to-noise ratio (SNR).

The BER of Eq. (4.8) used a SNR twice that in Eq. (3.117) as the correlated binary signal is $E(t) \pm e^{j\theta_e}E(t-T)$, uses two time slots, and doubles the energy per symbol. While difficult to prove analytically, from numerical results, the BER of Eq. (4.5) and Eq. (4.8) are the same.

From Eq. (4.8), the BER is independent of the sign of the phase error. In later parts of this letter, only the results of positive phase error are shown. Figure 4.1 show the BER as a function of SNR ρ_s for a DPSK signal with phase errors of 10∘, 20∘, 30∘, and 40∘. Fig. 4.1 also shows the error probability with no phase error of Eq. (3.103). Fig. 4.2 shows the SNR penalty as a function of phase error for DPSK signal. The SNR penalty is calculated for a BER of 10^{-9}, corresponding to a required SNR of 20 (13 dB).

The curve of SNR penalty of a DPSK signal in Fig. 4.1 has insignificant difference with the corresponding curves in (Kim and Winzer, 2003, Fig. 3) (Bosco and Poggiolini, 2003, Fig. 2) (Winzer and Kim, 2003, Fig.5) (required the adjusting of x-axis). The phase error for a SNR penalty of 1 dB is about 16∘ (or 4.5% of 360∘) for a DPSK signal. In all of (Bosco and Poggiolini, 2003, Kim and Winzer, 2003, Winzer and Kim, 2003), the phase error of 1-dB SNR penalty is about 4 to 5% from simulation or analysis. With narrow bandwidth and from (Bosco and Poggiolini, 2003), the SNR penalty due to phase error is more or less independent of the optical filter before the interferometer. For SNR penalty less than 2 dB and from (Winzer and Kim, 2003), the SNR penalty due to phase error is more or less independent

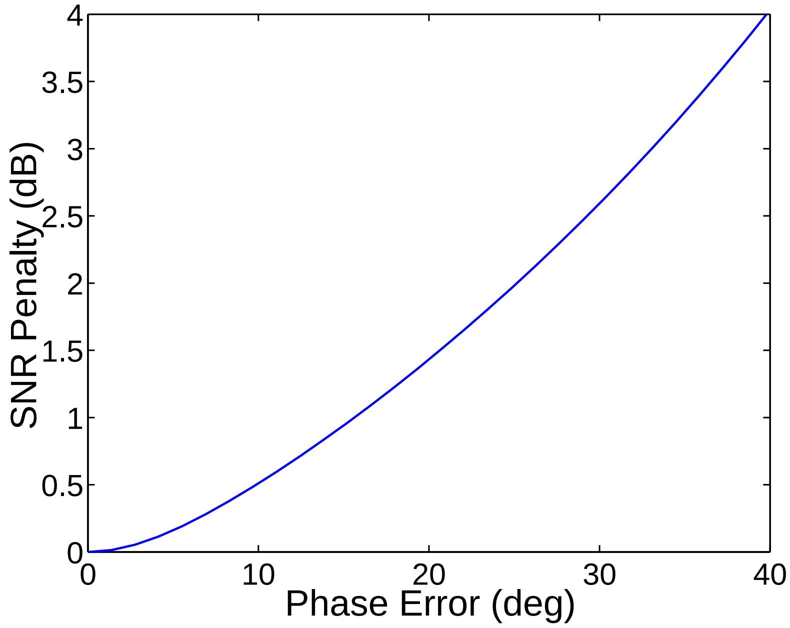

Figure 4.2: SNR penalty as a function of interferometer phase error for DPSK signals

of the electrical filtering after the balanced receiver. Just as with the theoretical results from (Bosco and Poggiolini, 2003, Kim and Winzer, 2003, Winzer and Kim, 2003), the SNR penalty of Fig. 4.2 is smaller than that from measurement (Kim and Winzer, 2003, Winzer and Kim, 2003). As explained in (Winzer and Kim, 2003), this discrepancy is probably due to the non-ideal signal source used in the experiment. The 10% (or 36○) mismatch of (Rohde et al., 2000) gives a penalty of about 3.5 dB.

The error probability of Eq. (4.8) assumes a matched filter, the typical cases of (Bosco and Poggiolini, 2003, Winzer and Kim, 2003). Within the matched filter, only the amplifier noise in the same polarization as the signal is considered, the typical cases of (Chinn et al., 1996, Humblet and Azizoğlu, 1991, Pires and de Rocha, 1992). The results are applicable to both return-to-zero (RZ) or non-return-to-zero (NRZ) line codes.

4.2.2 Phase Error in CPFSK Signals

In differential detection of CPFSK signal of Fig. 3.9, without noise, the phase difference at the output of the delay-and-multiplier circuit is

$$\Delta\phi_{\pm} = \omega_{IF}\tau \pm \pi\Delta f\tau. \tag{4.9}$$

In the phase difference of Eq. (4.9), there two types of equivalent phase error of $\exp(\omega_{\mathrm{IF}}\tau) \neq \pm j$ and $\Delta f\tau \neq 1/2$. The consequence of either case provides a phase error as the difference to the phase of $\pi/2$. The error probability is the same as that of Eq. (4.8) with, for example,

$$\theta_e = \pi\left(\frac{1}{2} - \Delta f\tau\right) \tag{4.10}$$

or $\exp(j\omega_{\mathrm{IF}}\tau) = \pm je^{j\theta_e}$. In either case, we have $e^{j\Delta\phi_{\pm}} = \pm e^{j\theta_e}$, $-\pi < \theta_e < \pi$.

When there are phase errors of both $\exp(\omega_{\mathrm{IF}}\tau) \neq \pm j$ and $\Delta f\tau \neq 1/2$. We can obtain two phase errors of $e^{j\theta_{e,\pm}} = e^{j\Delta\phi_{\pm}}$. The error probability of CPFSK signal is equal to the average of the error probability given by Eq. (4.8) with phase error of $\theta_{e,\pm}$, respectively.

4.3 Laser Phase Noise

For coherent optical communication, especially those using synchronous detection with phase tracking, the laser sources for both transmitter and local oscillator (LO) must be "coherent". The phase fluctuation or incoherent of a laser limits the sensitivity of a coherent optical communication systems. Semiconductor lasers widely used in communication systems are not as coherent as other types of laser source. From the semiclassical theory of semiconductor laser noise theory of Sec. 2.2.3, given by Eq. (2.41), the laser linewidth is broadened by a factor of $1 + \alpha^2$ compared with the Schawlow-Townes formula of Eq. (2.40), where α is the linewidth enhancement factor. With low facet reflectivity and short laser cavity, even with the linewidth enhancement, the Schawlow-Townes formula also gives a large linewidth for semiconductor laser. In here, the impact of laser phase noise to a coherent optical signal will be analyzed in details.

Ignored the effect of laser relaxation oscillation, the instantaneous frequency of a laser is assumed to be a white Gaussian noise. The frequency noise of the laser, the same as Eq. (2.39), has a spectral density of

$$S_{\phi_n}(f) = \frac{\Delta f_L}{2\pi f^2}. \tag{4.11}$$

where Δf_L is the full-width-half-maximum (FWHM) linewidth of the Lorentzian line-shape of Eq. (2.37)

$$S_{\phi_n}(f) = \frac{\Delta f_L^2}{\Delta f_L^2 + 4f^2}. \tag{4.12}$$

From Sec. 2.2.3, the phase of the semiconductor laser can be modeled as a Wiener process with the variance parameter of

$$\sigma_{n_\phi}^2 = 2\pi \Delta f_L, \tag{4.13}$$

and autocorrelation function of

$$E\left\{\phi_n(t_1)\phi_n(t_2)\right\} = \sigma_{n_\phi}^2 \min(t_1, t_2). \tag{4.14}$$

Both the spectral density of Eq. (4.11) and the line-shape of Eq. (4.12) are for a single laser. When two lasers are beating together in either homodyne or heterodyne system, the sum of the linewidth of both lasers becomes the linewidth at the immediate frequency (IF). For homodyne and heterodyne systems, the linewidth of Δf_L the sums of the linewidth of both transmitter laser and local oscillator (LO) laser. For direct-detection system, the linewidth of Δf_L is assumed to be that of the transmitter only.

The potential limitation of laser linewidth to coherent system was first studied by Yamamoto and Kimura (1981) and observed by Favre and LeGuen (1982), Kikuchi et al. (1983), Tamburrini et al. (1983). There were many follow-up studies on the topics at outline later.

4.3.1 Impact to PSK Signals

A PSK signal is demodulated using the receiver schematically shown in Fig. 1.3, either using a homodyne or heterodyne receiver. The phase-locked loop (PLL) of Fig. 1.3 comes with many different architecture. The simplest PLL may be the square loop for binary PSK in which a square-law device is used to generate a carrier frequency at $2f_{\mathrm{IF}}$. However, the squaring operation leads to noise enhancement that increase the noise power level at the input to the PLL and results in an increase of the variance of phase error (Proakis, 2000).

A decision-directed (or decision-feedback, decision-driven) PLL is shown in Fig. 4.3. A quadrature receiver of Fig. 3.4 is used in Fig. 4.3 to provide both the data and the phase error. For binary PSK signal, before the decision error, the output is

$$\frac{1}{2}[A(t) + n_1(t)] \cos\phi_e - \frac{1}{2} n_2(t) \sin\phi_e \tag{4.15}$$

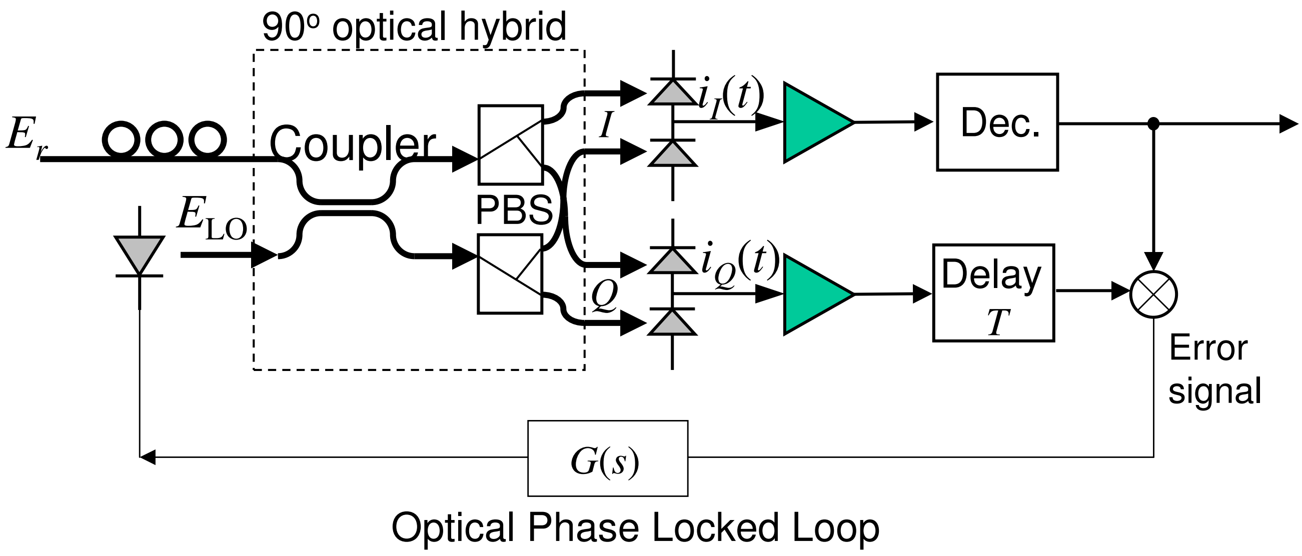

Figure 4.3: A decision-directed phase-locked loop to demodulate binary phase-shift keying signal

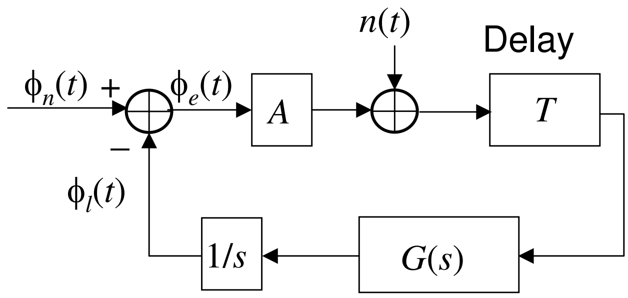

Figure 4.4: A linearized model of the PLL of Fig. 4.3

where ϕ_e is the phase error at the PLL. Without decision error, the output of the upper branch is $A_s(t) = \pm A$ after the decision circuit. The output of the lower branch is (Proakis, 2000)

$$\frac{1}{2}[A_s(t) + n_1(t)] \sin \phi_e - \frac{1}{2} n_2(t) \cos \phi_e. \tag{4.16}$$

The error signal is thus

$$e(t) = \frac{1}{2} A_s^2(t) \sin \phi_e + \frac{1}{2} A_s(t)[n_1(t) \sin \phi_e - n_2(t) \cos \phi_e] \tag{4.17}$$

Other than the noise term, the phase error is contained in $\frac{1}{2} A_s^2(t) \sin \phi_e$.

Figure 4.4 shows a linearized model of the PLL of Fig. 4.3. In practice, the parameter of Fig. 4.4 is $A = E\{A_s^2(t)/2\}$ and $n(t) = A_s(t) n_2(t)/2$. For simplicity without changing the SNR, we can assume that $A = |A_s(t)|$ with $A_s(t) = \pm A$ and $n(t) = n_2(t)$. In the linearized model of Fig. 4.3, the LO laser is modeled as an integrator of $1/s$ with $s = j2\pi f$. For a second-order PLL, the loop filter is $G(s) = K(s + a)/s$ where K includes the gain of the LO laser. The transfer function of the second-order loop is defined as $\phi_l(s)/\phi_n(s)$ as the ratio of the response of the $\phi_l(t)$ to $\phi_n(t)$. The closed-loop transfer function, expressed in terms of the loop filter $G(s)$ is than

$$H(s) = \frac{\phi_l(s)}{\phi_n(s)} = \frac{AKG(s)e^{-sT}}{s + AKG(s)e^{-sT}}. \tag{4.18}$$

For small T such that the term of e^{-sT} is equal to unity, we obtain

$$H(s) = \frac{AK(s+a)}{s^2 + AKs + AKa} = \frac{\omega_n^2 + 2\zeta\omega_n s}{\omega_n^2 + 2\zeta\omega_n s + s^2}. \tag{4.19}$$

where $\omega_n^2 = AKa$ and $\zeta = \frac{1}{2}\sqrt{AK/a}$, corresponding to the cut-off frequency and damping factor of a second-order transfer function, respectively. With $e^{-sT} \neq 1$, we obtain

$$H(s) = \frac{2\zeta\omega_n s + \omega_n^2}{s^2 e^{sT} + 2\zeta\omega_n s + \omega_n^2}. \tag{4.20}$$

The phase error of $\phi_e(t)$ has two components arising from $n(t)$ and the phase noise of $\phi_n(t)$, respectively. In the linearized analysis, we obtain

$$\phi_e(t) = \frac{1}{A} n(t) \otimes h(t) + \phi_n(t) \otimes [1 - h(t)] \tag{4.21}$$

where $\otimes$ denotes convolution. The spectral density of $\phi_e(t)$ is

$$S_{\phi_e}(f) = \frac{S_N(f)}{A^2} |H(j2\pi f)|^2 + S_{\phi_n}(s) |1 - H(j2\pi f)|^2. \tag{4.22}$$

The phase error variance is

$$\sigma_{\phi_e}^2 = \frac{N_0}{A^2} \int_0^\infty |H(j2\pi f)|^2 \mathrm{d}f + 2\int_0^\infty S_{\phi_n}(f) |1 - H(j2\pi f)|^2 \mathrm{d}f \tag{4.23}$$

where $N_0 = 2\sigma_n^2 T$ is the spectral density of $n(t)$.

The short-delay approximation of $e^{-sT} \approx 1$

When $e^{-sT} \approx 1$, we obtain

$$B_n = \int_0^\infty |H(j2\pi f)|^2 \mathrm{d}f = \frac{\omega_n}{8\zeta}(1 + 4\zeta)^2. \tag{4.24}$$

In the usual case of $\zeta = 1/\sqrt{2}$, we obtain

$$B_n = \frac{3\omega_n}{4\sqrt{2}} = 0.53\omega_n. \tag{4.25}$$

The tracking error function is

$$|1 - H(j2\pi f)|^2 = \frac{(2\pi f/\omega_n)^4}{[1 + (2\pi f/\omega_n)^2]^2 + (4\zeta\pi f/\omega_n)^2}. \tag{4.26}$$

With the phase error spectrum of Eq. (4.11), we obtain

$$\int_0^\infty S_{\phi_n}(f) |1 - H(j2\pi f)|^2 \mathrm{d}f = \frac{\Delta f_L}{2\omega_n} \int_0^\infty \frac{x^2}{1 + 2x^2(2\zeta^2 - 1) + x^4} \mathrm{d}x = \frac{\pi}{4\zeta} \frac{\Delta f_L}{\omega_n} \tag{4.27}$$

For $\zeta = 1/\sqrt{2}$, we obtain

$$\sigma_{\phi_e}^2 = \frac{0.53\omega_n T}{\rho_s} + 2.22 \frac{\Delta f_L}{\omega_n}. \tag{4.28}$$

The optimal bandwidth to minimize the phase error variance is

$$\omega_{n,\mathrm{opt}} = 2.04 \sqrt{\frac{\Delta f_L \rho_s}{T}} \tag{4.29}$$

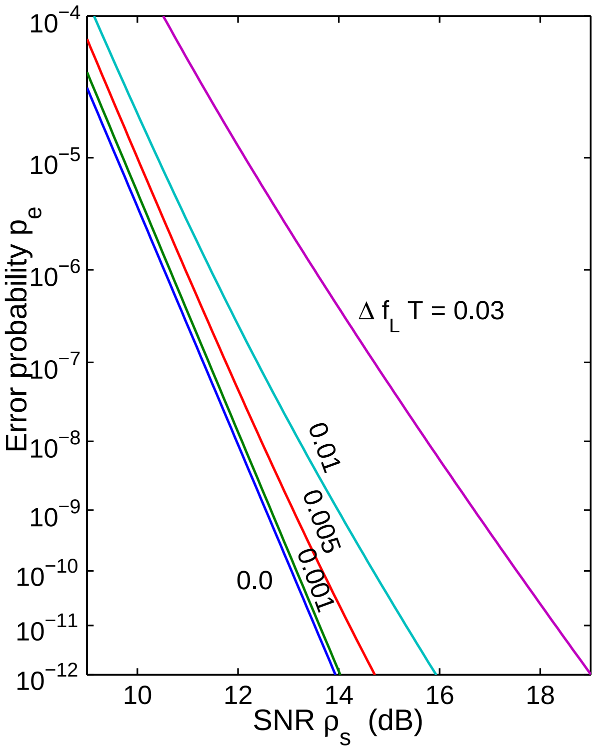

Figure 4.5: The error probability of binary PSK signal with laser phase noise

to give an minimum phase error variance of

$$\sigma^2_{\phi_e,\min} = 2.17\sqrt{\frac{\Delta f_L T}{\rho_s}}. \tag{4.30}$$

For general case, we can obtain

$$\sigma^2_{\phi_e,\min} = \sqrt{\pi\frac{\Delta f_L T}{\rho_s}\left(1+\frac{1}{4\zeta^2}\right)}. \tag{4.31}$$

With phase error, the error probability of a PSK signal is

$$p_e = \frac{1}{2}\int_{-\pi}^{\pi} \mathrm{erfc}\left(\sqrt{\rho_s}\cos\phi_e\right) p_{\Phi_e}(\phi_e)\mathrm{d}\phi_e \tag{4.32}$$

where $p_{\Phi_e}(\phi_e)$ is the probability density of the phase error. Using the series expansion of the Appendix, similar to Eq. (54), we can obtain

$$p_e = \frac{1}{2} - \exp\left(-\frac{\rho_s}{2}\right)\sqrt{\frac{\rho_s}{\pi}}\sum_{k=0}^{\infty}\frac{(-1)^k}{2k+1}\left[I_k\left(\frac{\rho_s}{2}\right)+I_{k+1}\left(\frac{\rho_s}{2}\right)\right]\exp\left(-\frac{(2k+1)^2}{2}\sigma^2_{\phi_e}\right), \tag{4.33}$$

if the phase error is assumed to be Gaussian distribution with a variance of $\sigma^2_{\phi_e}$.

Using the minimum phase error variance of Eq. (4.31), Figure 4.5 shows the error probability of binary PSK signal calculated using Eq. (4.33). The error probability of Fig. 4.5 is shown for several different values of normalized combined laser linewidth of $\Delta f_L T$. Figure 4.6 shows the SNR penalty of binary PSK signal as a function of the normalized combined laser linewidth of $\Delta f_L T$. In additional to use the optimal bandwidth of Eq. (4.29), the SNR penalty of Fig. 4.6 is also calculated with $\omega_n T$ is 0.1 and 0.05 of 2π.

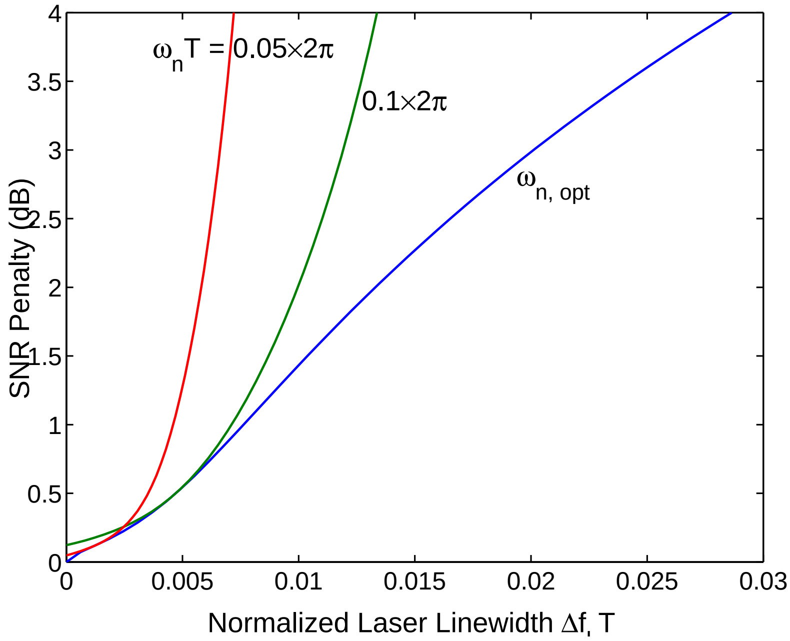

Figure 4.6: The SNR penalty of binary PSK signal as a function of laser linewidth for PLL without delay.

For an 1-dB SNR penalty, from Fig. 4.6, the normalized laser linewidth of $\Delta f_L T$ must be less 7.7×10^{-3}. The same as (Kazovsky, 1986b), a normalized laser linewidth of $\Delta f_L T$ of about 5×10^{-3} gives a SNR penalty of 0.5 dB.

Accurate Results of $e^{-sT} \neq 1$

For large normalized laser linewidth of $\Delta f_L T$, the PLL must have a bandwidth comparable to the data rate of $1/T$. With a large PLL bandwidth, the approximation of $e^{-sT} = 1$ is required to be verified. Without the approximation of $e^{-st} \neq 1$, the variance of phase error is equal to

$$\sigma^2_{\phi_e} = \frac{\omega_n}{2\pi\rho_s} \int_0^\infty \frac{1 + (2\zeta x)^2}{D(x)} \mathrm{d}x + \frac{2\Delta f_L}{\omega_n} \int_0^\infty \frac{x^2}{D(x)} \mathrm{d}x \tag{4.34}$$

where $D(x) = [1 - x^2 \cos(\alpha x)]^2 + [2\zeta x - x^2 \sin(\alpha x)]^2$ and $\alpha = \omega_n T$. The phase error variance of Eq. (4.34) is very complicated and it is difficult to find the parameters to optimize the system analytically.

Figure 4.7 shows the SNR penalty of binary PSK signal calculated using Eq. (4.34) with $\omega_n T/2\pi$ equal to 0.01 to 0.07 and $\zeta = 1/sqrt2$. With minimum PLL delay of T, the maximum normalized linewidth of $\Delta f_L T$ must be less than 2×10^{-3} for a SNR penalty less than 1 dB. This is substantial less than the 5×10^{-3} requirement of Fig. 4.6 for PLL without delay. The optimal PLL bandwidth is $\omega_n T/2\pi \approx 0.04$. In both Fig. 4.6 and Fig. 4.7, the standard deviation of phase error is about 11.5° for a SNR penalty of 1 dB.

For a 10-Gb/s system, the maximum normalized linewidth of $\Delta f_L T$ of 2×10^{-3} gives a combined laser linewidth of 20 MHz or 10 MHz linewidth for either transmitter or LO laser. Most DFB laser has a linewidth in the order several MHz right now. The combined linewidth of both transmitter and receiver is not likely limited by laser linewidth. Unlike low speed system in early systems, current 10-Gb/s is not likely to be limited by laser linewidth.

The system limited by amplifier noise, the effects of laser phase noise to heterodyne and homodyne receiver is the same. For system limited by shot noise, the analysis here also applies to heterodyne system (Kazovsky, 1986b, Norimatsu and Iwashita, 1992). The analysis here followed that of Kazovsky (1986b),

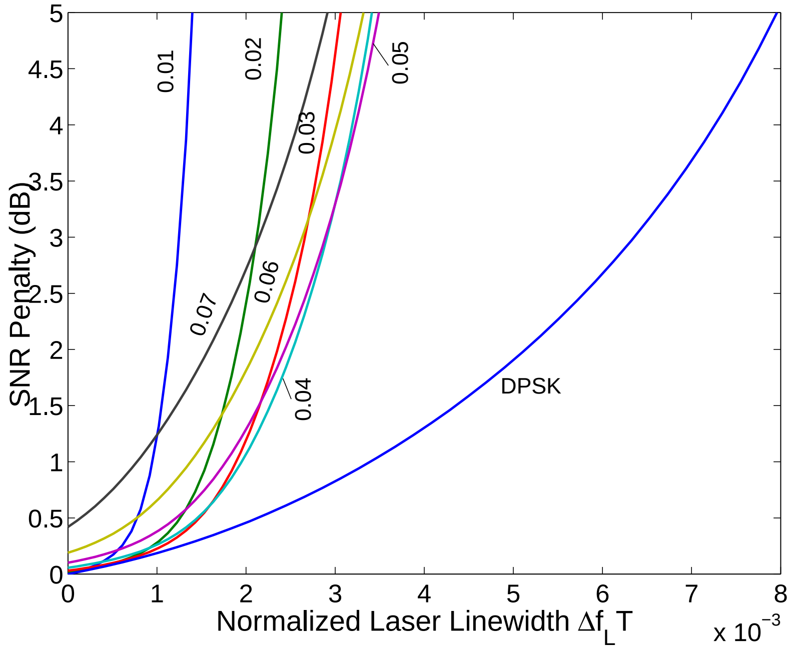

Figure 4.7: The SNR penalty of binary PSK signal as a function of laser linewidth for PLL with delay of T. The labels of each curve are $\omega_n T/2\pi$.

Spilker, Jr. (1977) but also taken into account the loop delay of T (Grant et al., 1987, Norimatsu and Iwashita, 1992).

The impact of phase error variance of PSK signal is well-known (Prabhu, 1976) and further analyzed by Glance (1986), Hodgkinson (1987), Kikuchi et al. (1984). The procedure of optimizing the PLL, especially decision-driven PLL, is the same as that in Kazovsky (1985, 1986b), Norimatsu and Ishida (1994), Norimatsu and Iwashita (1991, 1992), Spilker, Jr. (1977).

Without decision feedback, the PLL of Fig. 4.3 is similar to a Costa loop. Costa loop was implemented for PSK signal by Norimatsu et al. (1990), Schöpflin et al. (1990). The performance of Costa loop is the same as square-loop with noise enhancement due to the square operation (Proakis, 2000). Most implementation of homodyne PLL receiver using the balanced PLL similar to Fig. 4.3 with or without decision feedback. Other than (Kahn, 1990, Sun and Ye, 1990), most implementation of the PLL of

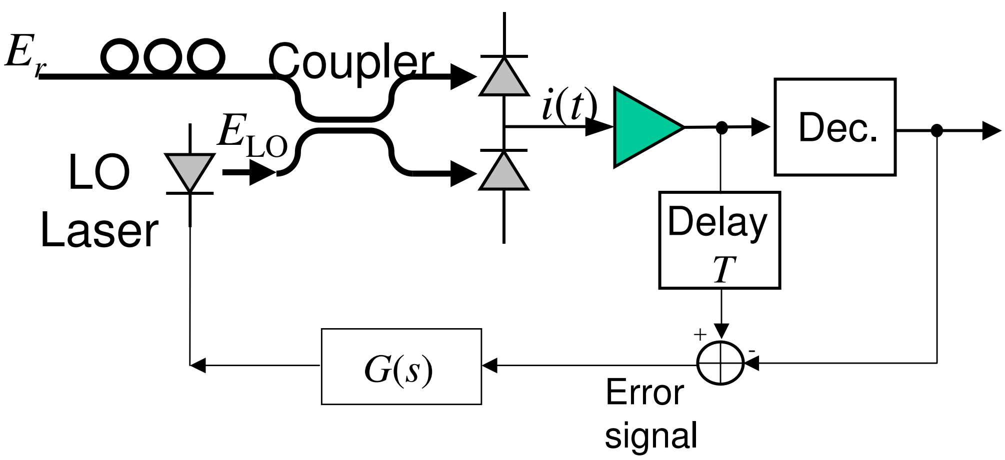

Figure 4.8: The balanced PLL to demodulate binary PSK signal.

Fig. 4.8 does not remove the data to phase error crosstalk (Altas and Kazovsky, 1990, Kahn, 1989, Kahn et al., 1990). Other than using a squared-loop or Costa loop, the implementation of the PLL of Fig. 4.8 required the usage of part of the signal to generate the error signal for the loop (Kahn, 1990, Kahn et al., 1990, Kazovsky, 1986a, Sun and Ye, 1990).

Because the signal splitting ratio of the coupler preceding the balanced receiver also affects the performance of the systems, the optimization of the PLL becomes very complicated for system dominated by shot noise (Kazovsky, 1985, 1986a). The balanced PLL of Fig. 4.3 is further complicated by the requirement to splitting the signal for data and phase locking (Huang and Wang, 1995, 1996). Homodyne system limited by shot noise has a very small linewidth requirement down to 10^{-5} the date rate.

In heterodyne PSK system, the effect of laser phase noise can be reduced by the recovery of a carrier with the same phase noise (Cheng and Okoshi, 1989, Chikama et al., 1990, Watanabe et al., 1989, 1992). When carrier is recovered using a band-pass filter, the bandwidth of the band-pass filter needs to pass the carrier with phase noise. A large filter bandwidth translates to larger phase error variance due to receiver noise than those based on PLL. Like homodyne PSK system, heterodyne PSK signal can be demodulated using PLL. (Kazovsky et al., 1990).

4.3.2 Impact to DPSK Signals

For a DPSK signal demodulated by a delay-and-multiplier circuit, the phase error due to laser phase noise in two consecutive symbol is equal to

$$\sigma^2_{\phi_e} = 2\pi\Delta f_L T. \tag{4.35}$$

There are two methods to calculate the error probability due to laser phase noise, the first method using an integration of similar to Eq. (4.32) of

$$p_e = \int_{-\pi}^{+\pi} p_e(\phi_e) p_{\Phi_e}(\phi_e) \mathrm{d}\phi_e \tag{4.36}$$

where $p_e(\phi_e)$ is the error probability of DPSK signal having an phase error of ϕ_e, the same as that of Eq. (4.8) with $\theta_e = \phi_e$. Similar to the series of Eq. (57) and Eq. (4.33), for Gaussian distributed phase error, the error probability of a DPSK signal with phase error is equal to

$$\begin{aligned} p_e &= \frac{1}{2} - \frac{\rho_s e^{-\rho_s}}{2} \sum_{k=0}^{\infty} \frac{(-1)^k}{2k+1} \left[I_k\left(\frac{\rho_s}{2}\right) + I_{k+1}\left(\frac{\rho_s}{2}\right) \right]^2 \\ &\qquad \times \exp\left[-(2k+1)^2 \pi \Delta f_L T \right]. \end{aligned} \tag{4.37}$$

Figure 4.9 shows the error probability of DPSK signal with laser phase noise. The SNR penalty of DPSK signal is already shown in Fig. 4.7 for comparison. From Fig. 4.7, a normalized linewidth $\Delta f_L T = 3.4 \times 10^{-3}$ gives a SNR of 1 dB for DPSK signal. The linewidth requirement of DPSK signals is 1.7 times that of PSK systems.

In heterodyne DPSK receiver, the linewidth of Δf_L is the overall linewidth from both transmitter and LO laser. In direct-detection DPSK receiver, the linewidth of Δf_L is the linewidth from the transmitter alone. For a 10-Gb/s heterodyne system, the linewidth of either transmitter and LO laser must be less than 17 MHz individually.

The analysis here for DPSK signals is the same as that of Nicholson (1984) by assuming that the filter after the delay-and-multiplier circuits do not further distort the signal and the usage of match IF filter. Jacobsen (1993), Jacobsen and Garrett (1987) further assumes that the IF filter is not a matched filter. The statistics of the filtered light with phase noise is found by Foschini and Vannucci (1988), Foschini et al. (1989) and used by Azizoğlu and Humblet (1991), Kaiser et al. (1993). Methods to analyze DPSK signal with phase noise was reviewed by Smith et al. (1995).

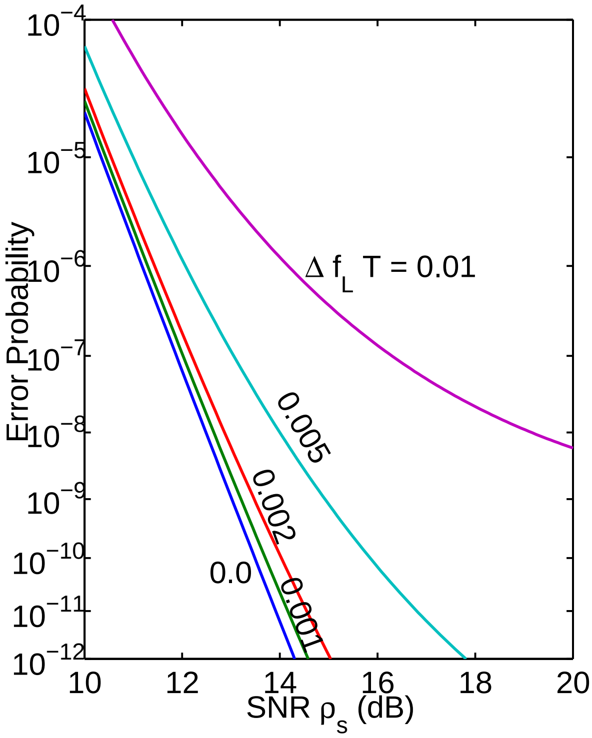

Figure 4.9: The error probability of DPSK signal with laser phase noise

4.3.3 Impact to Other Signals

The impact of laser phase noise to MSK signal is identical to that of DPSK signal if differential demodulator with a delay of the symbol time of T is used. The error probability of MSK signal with laser phase noise is the same as that of Eq. (4.37). For the general case of CPFSK signal, the error probability is the combination of Eq. (4.8) and Eq. (4.37) of

$$\begin{aligned} p_e &= \frac{1}{2} - \frac{\rho_s e^{-\rho_s}}{2} \sum_{k=0}^{\infty} \frac{(-1)^k}{2k+1} \left[I_k\left(\frac{\rho_s}{2}\right) + I_{k+1}\left(\frac{\rho_s}{2}\right)\right]^2 \\ &\quad \times \exp\left[-(2k+1)^2 \pi \Delta f_L \tau\right] \cos[(2k+1)\theta_e], \end{aligned} \tag{4.38}$$

where θ_e is that of Eq. (4.10) and τ is the delay for the differential demodulator of the CPFSK receiver of Fig. 3.9. The performance of CPFSK signal is analyzed followed the methods of Emura et al. (1990), Iwashita and Matsumoto (1987).

Phase noise also degrades dual-detected FSK signal or envelop detected ASK signal. However, most analysis showed that those systems can tolerate a laser linewidth up to at least 10% of the data rate (Corvaja et al., 1992, Foschini et al., 1988, Garrett et al., 1990, Greenstein et al., 1989, Kazovsky and Tonguz, 1990). Currently, most communication systems use semiconductor DFB laser with a linewidth of several MHz. For high-speed transmission with a Gb/s of data rate, the linewidth of several Hz does not affect the performance of both ASK and FSK system.

4.4 Fiber Dispersion

4.5 Polarization-Mode Dispersion

4.6 Summary

[A]Phase Distribution of Gaussian Random Variables

With only additive Gaussian noise, the baseband representation of the received signal is

$$s(t) = A + n(t), \tag{39}$$

where A is a real-number representing the transmitted signal and $n(t)$ is complex Gaussian noise with $n(t) = n_1(t) + jn_2(t)$. For a noise variance of $E\{n_1^2(t)\} = E\{n_2^2(t)\} = \sigma_n^2$, the p.d.f. of the received signal is

$$p(x_1, x_2) = \frac{1}{2\pi\sigma_n^2} \exp\left[-\frac{(x_1 - A)^2 + x_2^2}{2\sigma_n^2}\right], \tag{40}$$

with characteristic function of

$$\Psi(\omega) = \exp\left(j\omega_1 A - \frac{1}{2}\sigma_n^2|\omega|^2\right). \tag{41}$$

where $\omega = \omega_1 + j\omega_2$ as a complex number.

The received signal can convert to polar representation of $s(t) = r(t)e^{j\theta_n(t)}$ with $x_1 = r(t)\cos\theta_n(t)$ and $x_2 = r(t)\sin\theta_n(t)$, we obtain the distribution of $r(t)$ and $\theta_n(t)$ as

$$\begin{aligned} p_{R,\Theta_n}(r,\theta) &= \frac{r}{2\pi\sigma_n^2} \exp\left(-\frac{(r\cos\theta - A)^2 + r^2\sin^2\theta}{2\sigma_n^2}\right) \\ &= \frac{r}{2\pi\sigma_n^2} \exp\left(-\frac{r^2 + A^2 + 2r\cos\theta}{2\sigma_n^2}\right). \end{aligned} \tag{42}$$

The distribution of the received amplitude R is (Rice, 1944, 1948)

$$p_R(r) = \int_{-\pi}^{+\pi} p_{R,\Theta_n}(r,\theta)\mathrm{d}\theta = \frac{r}{\sigma_n^2} \exp\left(-\frac{r^2 + A^2}{2\sigma_n^2}\right) I_0\left(\frac{rA}{\sigma_n^2}\right) \tag{43}$$

as the Rice distribution, where $I_0(\cdot)$ is zero-order modified Bessel function of first kind given by $I_0(z) = \frac{1}{\pi}\int_0^\pi e^{z\cos\theta}\mathrm{d}\theta$ (Gradshteyn and Ryzhik, 1980, §8.431).

The received intensity is $Y = R^2$ with a noncentral chi-square (χ^2) distribution of

$$p_Y(y) = \frac{1}{2\sigma_n^2} \exp\left(-\frac{y + A^2}{2\sigma_n^2}\right) I_0\left(\frac{\sqrt{y}A}{\sigma_n^2}\right). \tag{44}$$

For phase modulation, the phase component of the received electric field has a distribution of

$$\begin{aligned} p_{\Theta_n}(\theta) &= \int_0^\infty p_{R,\Theta_n}(r,\theta)\mathrm{d}r \\ &= \frac{1}{2\pi}e^{-\rho_s} + \sqrt{\frac{\rho_s}{4\pi}}\cos\theta e^{-\rho_s\sin^2\theta}\mathrm{erfc}\left(-\sqrt{\rho_s}\cos\theta\right). \end{aligned} \tag{45}$$

The distribution of Eq. (45) is a function of $\cos\theta$ and thus a even periodic function with a period of 2π. We can expand the p.d.f. of Eq. (45) as a Fourier series of

$$p_{\Theta_n}(\theta) = \frac{1}{2\pi}\sum_{m=-\infty}^{\infty} c_m \exp(-jm\theta). \tag{46}$$

It is difficult to find the coefficients of c_m directly from the p.d.f. of Eq. (45), we can calculate the coefficients according to

$$\begin{aligned} c_m &= \int_{-\pi}^{\pi} p_{\Theta_n}(\theta) e^{jm\theta} \mathrm{d}\theta \\ &= \int_0^{\infty} \int_{-\pi}^{\pi} p_{R,\Theta_n}(r,\theta) e^{jm\theta} \mathrm{d}\theta \mathrm{d}r, \quad m \geq 0, \end{aligned} \tag{47}$$

and $c_{-m} = c_m$. Using Gradshteyn and Ryzhik (1980, §8.431), we obtain

$$\int_{-\pi}^{\pi} p_{R,\Theta_n}(r,\theta) e^{jm\theta} \mathrm{d}\theta = \frac{r}{\sigma_n^2} \exp\left(-\frac{r^2 + A^2}{2\sigma_n^2}\right) I_m\left(\frac{rA}{\sigma_n^2}\right). \tag{48}$$

Using Gradshteyn and Ryzhik (1980, §6.614, §9.220), the integration of Eq. (48) over amplitude r is equal to

$$\begin{aligned} c_m &= \frac{\rho_s^{\frac{m}{2}}}{m!} \Gamma\left(\frac{m}{2} + 1\right) {}_1F_1\left(\frac{m}{2}; m+1; -\rho_s\right) \\ &= \frac{\sqrt{\pi \rho_s}}{2} e^{-\rho_s/2} \left[I_{\frac{m-1}{2}}\left(\frac{\rho_s}{2}\right) + I_{\frac{m+1}{2}}\left(\frac{\rho_s}{2}\right)\right], \end{aligned} \tag{49}$$

where $\Gamma(\cdot)$ is the Gamma function, ${}_1F_1(a; b; \cdot)$ is the confluent hypergeometric function of the first kind , and $I_k(\cdot)$ is the k-th order modified Bessel function of the first kind. The p.d.f. of Eq. (45) is equal to

$$p_{\Theta_n}(\theta) = \frac{1}{2\pi} + \frac{e^{-\frac{\rho_s}{2}}}{2} \sqrt{\frac{\rho_s}{\pi}} \sum_{m=1}^{\infty} \left[I_{\frac{m-1}{2}}\left(\frac{\rho_s}{2}\right) + I_{\frac{m+1}{2}}\left(\frac{\rho_s}{2}\right)\right] \cos(m\theta). \tag{50}$$

The series representation of the phase distribution Eq. (50) can be found in Middleton (1960, §9.2-2) and Blachman (1981, 1988), Jain (1974), Jain and Blachman (1973), Prabhu (1969). The conversion from hypergeometric function to Bessel function is given by Blachman (1981, 1988), Jain (1974), Jain and Blachman (1973), Prabhu (1969).

The variance of the phase of amplifier noise is equal to

$$\begin{aligned} \sigma_{\Theta_n}^2 &= 2 \int_0^{\pi} \theta^2 p_{\Theta_n}(\theta) \mathrm{d}\theta \\ &= \frac{\pi^2}{3} + 2e^{-\frac{\rho_s}{2}} \sqrt{\pi \rho_s} \sum_{m=1}^{\infty} \frac{(-1)^m}{m^2} \left[I_{\frac{m-1}{2}}\left(\frac{\rho_s}{2}\right) + I_{\frac{m+1}{2}}\left(\frac{\rho_s}{2}\right)\right]. \end{aligned} \tag{51}$$

For high SNR, the p.d.f. of Eq. (45) can be approximated as

$$p_{\Theta_n}(\theta) \approx \sqrt{\frac{\rho_s}{\pi}} \cos\theta e^{-\rho_s \sin^2\theta} \tag{52}$$

with variance of

$$\sigma_{\Theta_n}^2 \approx \frac{1}{2\rho_s}. \tag{53}$$

Figure 10 shows the exact phase variance of Eq. (51) and the approximated phase variance of Eq. (53) as a function of SNR ρ_s. In high SNR of $\rho_s > 10$ dB, the exact [Eq. (51)] and approximated [Eq. (53)] phase variance are almost the same.

Figure 11 shows the p.d.f. of $p_{\Theta_n}(\theta)$ [either Eq. (45) or Eq. (50)] for a SNR of $\rho_s = 11, 18, 25$ (10.4 12.6 14.0 dB). The zero-mean Gaussian approximation with a variance of Eq. (53) is also plotted in Fig. 11

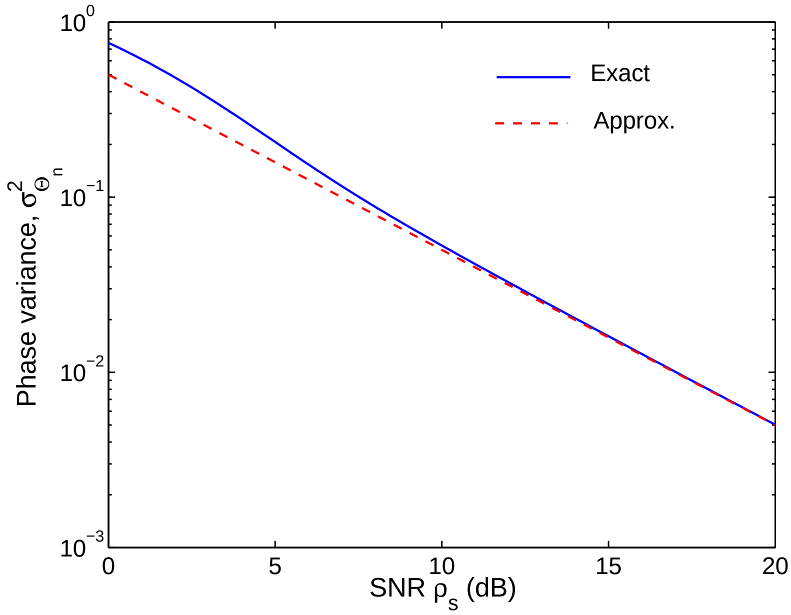

Figure 10: The phase variance of $\sigma^2_{\Theta_n}$ as a function of SNR ρ_s.

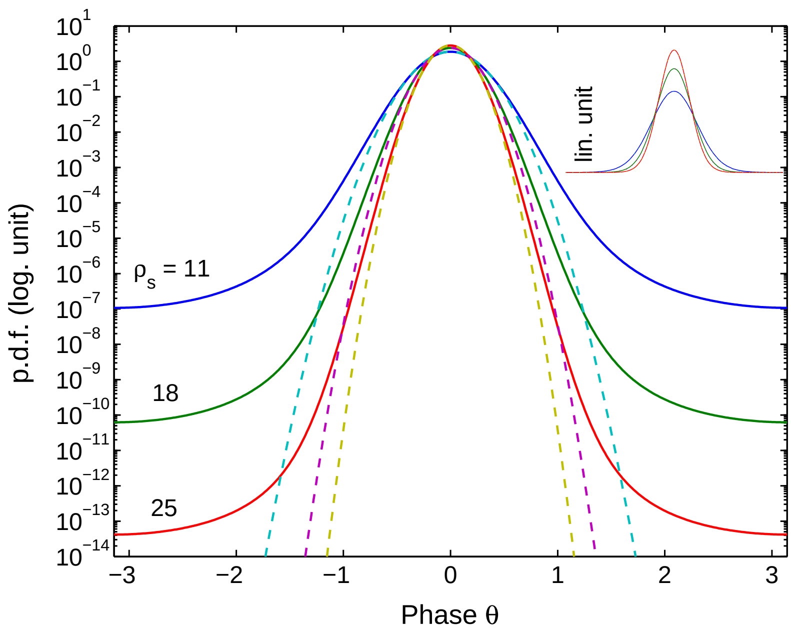

Figure 11: The p.d.f. of $p_{\Theta_n}(\theta)$ as comapred with the Gaussian approximation.

for comparison. Figure 11 plots in logarithmic scale to show the difference in the tail between the exact p.d.f. and Gaussian approximation. An inset plots the p.d.f. in linear scale. In the linear scale inset, the exact and approximated p.d.f. overlaps with each other and has not observable difference. While the phase distribution of $p_{\Theta_n}(\theta)$ [either Eq. (45) or Eq. (50)] is the same as Gaussian distribution in linear scale, Gaussian distribution cannot be used if a tail probability is interested. For optical communications interest in an error probability of 10^{-9} or lower, the tail probability is essential to evaluate the error probability.

Based on the series expansion of Eq. (50), the error probability of binary PSK signal [see Eq. (3.76)] is also equal to

$$\begin{aligned} p_e &= 1 - \int_{-\frac{\pi}{2}}^{\frac{\pi}{2}} p_{\Theta_n}(\theta) \mathrm{d}\theta \\ &= \frac{1}{2} - \frac{e^{-\frac{\rho_s}{2}}}{2} \sqrt{\frac{\rho_s}{\pi}} \sum_{m=1}^{\infty} \frac{2\sin(m\pi/2)}{m} \left[I_{\frac{m-1}{2}}\left(\frac{\rho_s}{2}\right) + I_{\frac{m+1}{2}}\left(\frac{\rho_s}{2}\right)\right] \\ &= \frac{1}{2} - \exp\left(-\frac{\rho_s}{2}\right) \sqrt{\frac{\rho_s}{\pi}} \sum_{k=0}^{\infty} \frac{(-1)^k}{2k+1} \left[I_k\left(\frac{\rho_s}{2}\right) + I_{k+1}\left(\frac{\rho_s}{2}\right)\right]. \end{aligned} \tag{54}$$

Because $\sin(m\pi/2) = 0$ for m as even number, the error probability of Eq. (54) is simplified.

From the factor of $(-1)^k$, the terms of Eq. (54) oscillate between positive and negative values. Although the summation of Eq. (54) converges, the calculation is numerically challenging for small error probability. Note that the multiplication factor of the summation is a small value in the order of $e^{-\frac{\rho_s}{2}}\sqrt{\rho_s}$, the summation has a value in the order of $e^{\frac{\rho_s}{2}}/\sqrt{\rho_s}$ for small error probability. For large SNR ρ_s, the summation has very large terms although the error probability is small. The error probability is the difference between 1/2 and a value a little bit smaller than 1/2. The series summation of Eq. (54) can be calculated to an error probability of 10^{-13} to 10^{-14} with an accuracy of three to four significant digits. Symbolic mathematical software can provide better accuracy by using variable precision arithmetic in the calculation of low error probability.

A DPSK signal is demodulated using the differential phase of

$$\Delta\Theta_n = \Theta_n(t) - \Theta_n(t-T), \tag{55}$$

where $\Theta_n(\cdot)$ is the phase of amplifier noise as a function of time and T is the symbol interval. The phases of $\Theta_n(t)$ and $\Theta_n(t-T)$ are two identical independently distributed random variables with p.d.f given by $p_{\Theta_n}(\theta)$ of either Eq. (45) and Eq. (50).

When two independently distributed random variables are summed (or subtracted) together, the characteristic function of the sum (or difference) is equal to the product of its individual characteristic functions. For the series expansion like Eq. (50), the sum has a Fourier coefficient that is the product of the corresponding Fourier coefficients. Based on the series expansion of Eq. (50), the differential phase of Eq. (55) has a p.d.f. of

$$p_{\Delta\Theta_n}(\theta) = \frac{1}{2\pi} + \frac{\rho_s e^{-\rho_s}}{4} \sum_{m=1}^{\infty} \left[I_{\frac{m-1}{2}}\left(\frac{\rho_s}{2}\right) + I_{\frac{m+1}{2}}\left(\frac{\rho_s}{2}\right)\right]^2 \cos(m\theta). \tag{56}$$

The error probability corresponding to Eq. (54) for DPSK signal [see Eq. (3.103) is

$$p_e = \frac{1}{2} - \frac{\rho_s e^{-\rho_s}}{2} \sum_{k=0}^{\infty} \frac{(-1)^k}{2k+1} \left[I_k\left(\frac{\rho_s}{2}\right) + I_{k+1}\left(\frac{\rho_s}{2}\right)\right]^2. \tag{57}$$

Comparing the error probability of Eq. (3.76) with Eq. (54) for PSK signal and Eq. (3.103) with Eq. (57) for DPSK signal, the series of Eq. (50) is not very useful for performance analysis of PSK signal. However, when the system has additive phase noise that is independent of the additive Gaussian noise, the series of Eq. (50) is very useful. The summed phase noise has Fourier coefficients that are the multiplication of the corresponding coefficients of each individual phase noise components. Using the series of Eq. (50), the error probability of PSK or DPSK signals was derived by Prabhu (1969) for multilevel signals, Jain (1974), Jain and Blachman (1973), Lindsey and Simon (1973), Prabhu (1976) with phase-locked loop noise, Blachman (1981) with phase error, Nicholson (1984) with laser phase noise, and Iwashita and Matsumoto (1987), Jacobsen and Garrett (1987) with phase error and laser phase noise.

Bibliography

Abbas, G. L., Chan, V. W. S., and Yee, T. K. (1985). A dual-detector optical heterodyne receiver for local oscillator noise suppression. *J. Lightwave Technol.*, LT-3(5):1110–1122.

Alexander, S. B. (1987). Design of wide-band optical heterodyne balanced mixer receivers. *J. Lightwave Technol.*, LT-5(4):523–537.

Altas, D. A. and Kazovsky, L. G. (1990). An optical PSK homodyne transmission experiment using 1320 nm diode-pumped Nd:YAG lasers. *IEEE Photon. Technol. Lett.*, 2(5):367–370.

Azizoğlu, M. and Humblet, P. A. (1991). Envelope detection of orthogonal signals with phase noise. *J. Lightwave Technol.*, 9(10):1398–1410.

Betti, S., de Marchis, G., and Iannone, E. (1995). *Coherent Optical Communication Systems.* Wiley, New York.

Blachman, N. M. (1981). The effect of phase error on DPSK error probability. *IEEE Trans. Commun.*, COM-29(3):364–465.

Blachman, N. M. (1988). Gaussian noise - part II: Distribution of phase change of narrow-band noise plus sinusoid. *IEEE Trans. Info. Theory*, 34(6):1401–1405.

Bosco, G. and Poggiolini, P. (2003). The effect of receiver imperfections on the performance of direct-detection optical systems using DPSK modulation. In *Optical Fiber Commun. Conf.* Optical Society of America, Washington, D.C. paper ThE6.

Cheng, Y. H. and Okoshi, T. (1989). Phase-noise-cancelling dual-frequency heterodyne optical fibre communication system. *Electron. Lett.*, 25(13):835–836.

Chikama, T., Watanabe, S., Naito, T., Onaka, H., Kiyonaga, T., Onoda, Y., Miyata, H., Suyama, M., Seino, M., and Kuwahara, H. (1990). Modulation and demodulation techniques in optical heterodyne PSK transmission systems. *J. Lightwave Technol.*, 8(3):309–322.

Chinn, S. R., Boroson, D. M., and Livas, J. C. (1996). Sensitivity of optically preamplified DPSK receivers with Fabry-Perot filters. *J. Lightwave Technol.*, 14(3):370–376.

Corvaja, R., Pierobon, G. L., and Tomba, L. (1992). Accurate performance evaluation of weakly coherent optical systems. *J. Lightwave Technol.*, 10(11):1665–1673.

Emura, K., Sato, K., Yamazaki, S., Murata, S., Shikada, M., and Minemura, K. (1990). Optimum system design for CPFSK heterodyne delay demodulation system with DFB LDs. *J. Lightwave Technol.*, 8(2):251–258.

Favre, F. and LeGuen, D. (1982). Effect of semiconductor phase noise on BER performance in an optical DPSK heterodyne-type experiment. *Electron. Lett.*, 18:964–965.

Foschini, G. J., Greenstein, L. J., and Vannucci, G. (1988). Noncoherent detection of coherent lightwave signals corrupted by phase noise. *IEEE Trans. Commun.*, 36(3):306–314.

Foschini, G. J. and Vannucci, G. (1988). Characteristing filtered light waves corrupted by phase noise. *IEEE Trans. Info. Theory*, 34(6):1438–1448.

Foschini, G. J., Vannucci, G., and Greenstein, L. J. (1989). Envelope statistics for filtered optical signals corrupted by phase noise. *IEEE Trans. Commun.*, 37(12):1293–1302.

Garrett, I., Bond, D. J., Waite, J. B., Lettis, D. S. L., and Jacobsen, G. (1990). Impact of phase noise in weakly coherent systems: a new and accurate approach. *J. Lightwave Technol.*, 8(3):329–337.

Glance, B. (1986). Performance of homodyne detection of binary PSK optical signals. *J. Lightwave Technol.*, LT-4(2):228–235.

Gradshteyn, I. S. and Ryzhik, I. M. (1980). *Table of Integrals, Series, and Products.* Academic Press, San Diego.

Grant, M. A., Michie, W. C., and Fletcher, M. J. (1987). The performance of optical phase-locked loops in the presence of nonnegligible loop propagation delay. *J. Lightwave Technol.*, LT-5(4):592–597.

Greenstein, L. J., Vannucci, G., and Foschini, G. J. (1989). Optical power requirements for detecting ook and fsk signals corrupted by phase noise. *IEEE Trans. Commun.*, 37(12):1275–1281.

Ho, K.-P. (2004). The effect of interferometer phase error on direct-detection DPSK and DQPSK signals. *IEEE Photon. Technol. Lett.*, 16(1):308–310.

Hodgkinson, T. (1987). Receiver analysis for synchronous coherent optical fiber transmission systems. *J. Lightwave Technol.*, LT-5(4):573–586.

Huang, S. and Wang, L. (1995). Optimum phase deviations between mark-and space-state bits in long-haul coherent communication systems with balanced PLL receivers. *J. Lightwave Technol.*, 13(10):1963–1970.

Huang, S. and Wang, L. (1996). Exact evaluation of laser linewidth requirements for optical PSK homodyne communication systems with balanced PLL receivers. *J. Lightwave Technol.*, 14(5):661–664.

Humblet, P. A. and Azizoğlu, M. (1991). On the bit error rate of lightwave systems with optical amplifiers. *J. Lightwave Technol.*, 9(11):1576–1582.

Iwashita, K. and Matsumoto, T. (1987). Modulation and detection characteristics of optical continuous phase FSK transmission system. *J. Lightwave Technol.*, LT-5(4):452–460.

Jacobsen, G. (1993). Performance of DPSK and CPFSK systems with significant post-detection filtering. *J. Lightwave Technol.*, 11(10):1622–163.

Jacobsen, G. and Garrett, I. (1987). Theory for optical heterodyne DPSK receivers with post-detection filtering. *J. Lightwave Technol.*, 5(4):478–484.

Jain, P. C. (1974). Error probabilities in binary angle modulation. *IEEE Trans. Info. Theory*, IT-20(1):36–42.

Jain, P. C. and Blachman, N. M. (1973). Detection of a PSK signal transmitted through a hard-limited channel. *IEEE Trans. Info. Theory*, IT-19(5):623–630.

Kahn, J. M. (1989). 1 Gbit/s PSK homodyne transmission system using phase-locked semiconductor lasers. *IEEE Photon. Technol. Lett.*, 1(10):340–342.

Kahn, J. M. (1990). BPSK homodyne detection experiment using balanced optical phase-locked loop with quantized feedback. *IEEE Photon. Technol. Lett.*, 2(11):840–843.

Kahn, J. M., Gnuack, A. H., Veselka, J. J., Korotky, S. K., and Kasper, B. L. (1990). 4-Gb/s PSK homodyne transmission system using phase-locked semiconductor lasers. *IEEE Photon. Technol. Lett.*, 2(4):285–287.

Kaiser, C. P., Shafi, M., and Smith, P. J. (1993). Analysis methods for optical heterodyne DPSK receivers corrupted by laser phase noise. *J. Lightwave Technol.*, 11(11):1820–1830.

Kazovsky, L. G. (1985). Decision-driven phase-locked loop for optical homodyne receivers: Performance analysis and laser linewidth requirements. *J. Lightwave Technol.*, LT-3(12):1238–1247.

Kazovsky, L. G. (1986a). Balanced phase-locked loops for optical homodyne receivers: Performance analysis, design considerations, and laser linewidth requirements. *J. Lightwave Technol.*, LT-4(2):182–195.

Kazovsky, L. G. (1986b). Performance analysis and laser linewidth requirements for optical PSK heterodyne communications systems. *J. Lightwave Technol.*, LT-4(4):415–425.

Kazovsky, L. G., Atlas, D. A., and Smith, R. W. (1990). Optical phase-locked PSK heterodyne experiment at 4 Gb/s. *IEEE Photon. Technol. Lett.*, 2(8):588–590.

Kazovsky, L. G. and Tonguz, O. K. (1990). ASK and FSK coherent lightwave systems: A simplified approximate analysis. *J. Lightwave Technol.*, 8(3):338–352.

Kikuchi, K., Okoshi, T., Nagamatsu, M., and Henmi, N. (1983). Bit-error rate of PSK heterodyne optical communication system and its degraduation due to spectral spread of transmitter and local oscillator. *Electron. Lett.*, 19:417–418.

Kikuchi, K., Okoshi, T., Nagamatsu, M., and Henmi, N. (1984). Degradation of bit-error rate in coherent optical communications due to spectral spread of the transmitter and the local oscillator. *J. Lightwave Technol.*, LT-2(6):1024–1033.

Kim, H. and Winzer, P. J. (2003). Robustness to laser frequency offset in direct-detection DPSK and DQPSK systems. *J. Lightwave Technol.*, 21(9):1887–1891.

Lindsey, W. C. and Simon, M. K. (1973). *Telecommunication Systems Engineering.* Prentice-Hall, Englewood Cliffs, N.J.

Middleton, D. (1960). *An Introduction to Statistical Comunication Theory.* McGraw-Hill, New York.

Nicholson, G. (1984). Probability of error for optical heterodyne DPSK system with quantum phase noise. *Electron. Lett.*, 20(24):1005–1007.

Norimatsu, S. and Ishida, O. (1994). Impact of flicker noise and random-walk noise on a phase-locked loop with finite propagation delay. *J. Lightwave Technol.*, 12(1):86–95.

Norimatsu, S. and Iwashita, K. (1991). PLL propagation delay-time influence on linewidth requirements of optical PSK homodyne detection. *J. Lightwave Technol.*, 9(10):1367–1375.

Norimatsu, S. and Iwashita, K. (1992). Linewidth requirements for optical synchronous detection systems with nonnegligible loop delay time. *J. Lightwave Technol.*, 10(3):341–349.

Norimatsu, S., Iwashita, K., and Noguchi, K. (1990). 10 Gbit/s optical PSK homodyne transmission experiments using external cavity DFB LDs. *Electron. Lett.*, 26(10):648–649.

Okoshi, T. and Kikuchi, K. (1988). *Coherent Optical Fiber Communications.* KTK Scientific, Tokyo.

Pires, J. J. O. and de Rocha, J. R. F. (1992). Performance analysis of DPSK direct detection optical systems in the presence of interferometric intensity. *J. Lightwave Technol.*, 10(11):1722–1730.

Prabhu, V. K. (1969). Error-rate considerations for digital phase-modulation systems. *IEEE Trans. Commun. Technol.*, COM-17(1):33–42.

Prabhu, V. K. (1976). PSK performance with imperfect carrier recovery. *IEEE Trans. Aerosp. Electron. Syst.*, AES-12(2):107–125.

Proakis, J. G. (2000). *Digital Communications.* McGraw Hill, New York, fourth edition.

Rice, S. O. (1944). Mathematical analysis of random noise. *Bell Syst. Tech. J.*, 23(3):283–332. vol. 24, no. 1, pp. 46–157, 1945.

Rice, S. O. (1948). Statistical properties of a sine wave plus random noise. *Bell Syst. Tech. J.*, 27(1):109–157.

Rohde, M., Caspar, C., Heimes, N., Konitzer, M., Bachus, E.-J., and Hanik, N. (2000). Robustness of DPSK direct detection transmission format in standard fibre WDM systems. *Electron. Lett.*, 36(17):1483–1484.

Ryu, S. (1995). *Coherent Lightwave Communication Systems.* Artec House, Boston.

Schöpflin, A., Kugelmeier, S., Gottwald, E., Felicio, D., and Fischer, G. (1990). PSK optical homodyne system with nonlinear phase-locked loop. *Electron. Lett.*, 26(6):395–396.

Smith, P. J., Shafi, M., and Kaiser, C. P. (1995). Optical heterodyne binary-DPSK systems: A review of analysis and performance. *IEEE J. Sel. Areas Commun.*, 13(3):557–568.

Spilker, Jr., J. J. (1977). *Digital Communications by Satellite.* Prentice Hall, Englewood Cliff, NJ.

Sun, L. and Ye, P. (1990). Optical homodyne receiver based on an improved balance phase-locked loop with the date-to-phaselock crosstalk suppression. *IEEE Photon. Technol. Lett.*, 2(9):678–679.

Tamburrini, M., Spano, S., and Piazzolla, S. (1983). Influence of semiconductor-laser phase noise on coherent optical communication systems. *Opt. Lett.*, 8(3):174–176.

Watanabe, S., Chikama, T., Naito, T., and Kuwahara, H. (1989). 560 Mbit/s optical PSK heterodyne detection using carrier recovery. *Electron. Lett.*, 25(9):588–590.

Watanabe, S., Naito, T., Chikama, T., and Kuwahara, H. (1992). Phase noise cancellation in a carrier recovered optical heterodyne receiver. *J. Lightwave Technol.*, 10(12):1963–1973.

Winzer, P. J. and Kim, H. (2003). Degradations in balanced DPSK receivers. *IEEE Photon. Technol. Lett.*, 15(9):1282–1284.

Yamamoto, Y. and Kimura, T. (1981). Coherent optical fiber transmission systems. *IEEE J. Quantum Electron.*, QE-17(6):919–935.

Yuen, H. P. and Chan, V. W. S. (1983). Noise in homodyne and heterodyne detection. *Opt. Lett.*, 8:177–179.